Different phosphorylation states of the anaphase promoting complex in response to antimitotic drugs: A quantitative proteomic analysis

Judith A. J. Steen*, Hanno Steen†, Ann Georgi‡, Kenneth Parker§, Michael Springer‡, Marc Kirchner¶, Fred Hamprecht¶, and Marc W. Kirschner‡‖

Departments of *Neurobiology and †Pathology, Harvard Medical School and Children's Hospital Boston, Boston, MA 02115; ‡Department of Systems Biology, Harvard Medical School, Boston, MA 02115; §Department of Neurology, Harvard Medical School and Brigham and Women's Hospital, Boston, MA 02115; and ¶Interdisciplinary Center for Scientific Computing, University of Heidelberg, D-69120 Heidelberg, Germany

Contributed by Marc W. Kirschner, October 16, 2007 (sent for review June 27, 2007)

The anaphase promoting complex (APC) controls the degradation of proteins during exit from mitosis and entry into S-phase. The activity of the APC is regulated by phosphorylation during mitosis. Because the phosphorylation pattern provides insights into the complexity of regulation of the APC, we studied in detail the phosphorylation patterns at a single mitotic state of arrest generated by various antimitotic drugs. We examined the phosphorylation patterns of the APC in HeLa S3 cells after they were arrested in prometaphase with taxol, nocodazole, vincristine, or monastrol. There were 71 phosphorylation sites on nine of the APC subunits. Despite the common state of arrest, the various antimitotic drug treatments resulted in differences in the phosphorylation patterns and phosphorylation stoichiometries. The relative phosphorylation stoichiometries were determined by using a method adapted from the isotope-free quantitation of the extent of modification (iQEM). We could show that during drug arrest the phosphorylation state of the APC changes, indicating that the mitotic arrest is not a static condition. We discuss these findings in terms of the variable efficacy of antimitotic drugs in cancer chemotherapy.

mass spectrometry | stable isotope free quantitation | prometaphase | cell cycle arrest

The anaphase-promoting complex (APC) is an essential ubiquitin ligase that coordinates events in the mitotic and G_1 phases of the cell cycle (1). The activity of the APC is regulated by two cofactors, CDC20 and CDH1 (2, 3), as well as by protein modifications including phosphorylation (4, 5). The APC is the target of the spindle checkpoint (6), a complex process that senses the fidelity of microtubule attachment to chromosomes before allowing chromatid separation and cell division to proceed. Improper microtubule attachment or chromosome misalignment on the spindle activates the formation of an inhibitory "supercomplex," consisting of the APC and a second complex, the mitotic checkpoint complex (MCC), which consists of a kinase BubR1, an inhibitor MAD2, and the APC activator CDC20 (1).

Phosphorylation is thought to be important in regulating the APC and several kinases are known to affect the spindle checkpoint machinery, including CDK1, PLK1 (7–9), BUB1, MPS1, BUBR1, and Aurora B (10). Furthermore, (*i*) the activation state of the APC is directly affected by phosphorylation (11–13); (*ii*) phosphorylation of the APC affects the binding of interacting partners such as CDC20 (2, 14–16); and (*iii*) the phosphorylation of CDC20 by BUB1 is also important for full inhibition of the APC by MAD2 (14).

The checkpoint machinery or related activities may be the indirect target of several anti-cancer therapies, including vinca alkaloids and taxanes, which are inhibitors of microtubule dynamics and are among the most effective anti-cancer agents (17–21). Although much is known about drug interactions with microtubules, why only some microtubule inhibitors are useful anti-cancer drugs is a puzzle: e.g., neither colchicine nor nocodazole finds use in tumor treatment. Therefore, a detailed understanding of the effects of anti-spindle drugs on the checkpoint and APC may provide clues to the development of even more effective therapies (22). In particular, because phosphorylation seems to be an important regulator of the checkpoint, a detailed monitoring of the phosphorylation state of the APC might prove informative (23).

Mass spectrometry has been used to map phosphorylation sites on the APC (4) from cells arrested with nocodazole. A total of 43 phosphorylation sites were found. Although this study highlighted the complexity and potential importance of the phosphorylation control of the APC, it provided little functional information: the sheer number of sites suggested that functional studies would be very difficult. Even a comprehensive set of point mutations at each phosphorylation site might not be enough to gain full functional understanding. Sites might act redundantly or dependently, and it would be prohibitively difficult to study all possible combinations. Furthermore, some sites might be quantitatively unimportant, whereas other sites might serve as unstable intermediates in important pathways. Although a complete analysis by mutation may be impossible, a quantitative and kinetic analysis might reveal important clues to APC's regulatory circuitry and provide new information about the dynamics of the arrested state and the action of antimitotic drugs.

Quantitative measurements of phosphorylation of a complex target are far from routine. Antibody-based approaches, using phosphorylation site specific antibodies/Western blot analysis and phosphopeptide specific enrichment strategies in combination with stable isotope labeling and mass spectrometric approaches cannot readily distinguish between changes in the degree of phosphorylation or changes in the level of a protein, which is a serious complication in the cell cycle where protein synthesis and degradation rates change rapidly. However, information about the stoichiometry of phosphorylation is critical. A 5-fold increase in signal could correspond to changes from 0.1% to 0.5% or to changes from 20% to 100% in phosphorylation. The former might be significant for an activating phosphorylation, but is probably insignificant for an inhibiting phosphorylation. Furthermore, low stoichiometries may be important if turnover is rapid, but that could only be evaluated in kinetic studies and such studies generally require an absolute measurement of stoichiometry. We recently developed a mass spectrometry technique, iQEM (isotope-free quantitation of

Author contributions: J.A.J.S., H.S., A.G., and M.W.K. designed research; J.A.J.S., H.S., and A.G. performed research; J.A.J.S., K.P., M.S., M.K., and F.H. contributed new reagents/analytic tools; J.A.J.S., H.S., K.P., and M.K. analyzed data; and J.A.J.S., H.S., and M.W.K. wrote the paper.

The authors declare no conflict of interest.

Freely available online through the PNAS open access option.

‖To whom correspondence should be addressed. E-mail: marc@hms.harvard.edu.

This article contains supporting information online at www.pnas.org/cgi/content/full/0709807104/DC1.

the extent of modification) (24), that addresses some of these problems. It allows analysis of phosphorylation stoichiometries without isotopic labeling and can be used to study the dynamics of modifications irrespective of the source of the protein material, even from whole tissue and/or biopsies.

In the work reported here, we comprehensively analyzed phosphorylation sites on the APC in response to a prometaphase arrest using various antimitotic drugs, several of them used in anti-cancer therapies. Subsequently, we applied concepts from iQEM to quantitatively determine the differences in phosphorylation stoichiometries of some of the sites upon treatment with the various antimitotic drugs. In addition we used iQEM to study the kinetics/temporal order of phosphorylation of the APC. Apart from identifying characteristic differences in phosphorylation profiles for the different spindle poisons we determined kinetics for several phosphorylation sites. This study demonstrates that mitotic arrest is not a unitary state; it is both dynamic and diverse.

Results

APC and Associated Proteins Are Heavily Phosphorylated in the Cell Cycle. Several strategies were tested to optimize identification of the APC phosphopeptides, a scheme of the strategy used is shown in supporting information (SI) Fig. 1 in *SI Appendix*. After immunoprecipitation, the APC was analyzed in several conditions: (M) double thymidine arrest followed by an 8-h release into mitosis; (G_1) double thymidine arrest released into G_1; (n) nocodazole mitotic arrest; (mn) monastrol mitotic arrest; (S) double thymidine arrest; (tl) 9 nM taxol mitotic arrest; (tm) 20 nM taxol mitotic arrest; (th) 40 nM taxol mitotic arrest; (vc) vincristine mitotic arrest. The drug treatments were selected to provide cells with similar distributions of cell cycle states. Not surprisingly, members of the spindle checkpoint complex were purified with the APC in cells treated with spindle poisons. Core APC and MCC proteins that were identified reproducibly in several experiments are listed in the SI Table 1 in *SI Appendix* (including obtained sequence coverage). Kinases, such as PLK1, Aurora kinase B, and CDK1 also coimmunoprecipitated with the APC complex (data not shown). A ubiquitin-conjugating E2 protein, E2S (UBE2S_HUMAN), that was not previously known to associate with the APC was found predominantly in G_1 and in the "mitosis" sample. Several other known interactors and substrates such as EMI1 and geminin were identified in the appropriate cell cycle phase. In addition, several other proteins of interest also copurified with the APC.

Undertaking a comprehensive phosphorylation analysis we were able to map 71 distinct phosphorylation sites under 9 different conditions. Table 1 shows a list of phosphorylation sites for the APC under the conditions described. The spectral evidence for the phosphorylation sites is shown in the SI Figs. 6 and 12–65 in *SI Appendix*. In four cases, the phosphorylation sites could not be unambiguously assigned to one amino acid residue. In these cases, two possible sites are indicated in the SI Figs. 12–65 in *SI Appendix*. Because there were differences in the sequence coverage from treatment to treatment, we could not assume that a phosphorylation that was not observed in a given condition was in fact not present. Unobserved sites are listed in Table 1 as absent (white) only if we saw the corresponding unphosphorylated peptide in at least one of the samples.

The Sites for Cells Undergoing Mitosis Are Different from Those Found in Nocodazole Arrest. The greatest number of phosphorylation sites appeared in drug-induced mitotic arrests. After nocodazole treatment, we found 43 phosphorylation sites, whereas in S- and G_1-phase we found only 2 and 5 sites, respectively. The data for S-phase and nocodazole treatment were in general agreement with the work of Kraft *et al*. (4). In a few cases, we differed with respect to the exact location of the phosphorylation site.

In most cell cycle studies, nocodazole arrest is used as a surrogate for the mitotic state. To test the validity of that assumption, we

Table 1. Phosphorylation sites mapped for the different APC subunits and related spindle checkpoint proteins

Protein	#	Phos. Motif	G1	S	M	mn	n	tl	tm	th	vc
APC1	1	KAFt118VDS									
	2	PPGs202PRE									
	3	LFGs233SRV									
	4	QGGt291PQN									
	5	HSRs341PSI									
	6	RAHS355PAL									
	7	GVHs362FSG									
	8	HNQs377PKR									
	9	RPSt530PLD									
	10	KPLs542KLL									
	11	VLLs555PVP									
	12	RDSs564KLH									
	13	LELs600NGS									
	14	GSLs688PVI									
	15	LzLs731PSE									
	16	EMNy1552GFH									
	17	GQLs1707YKE									
APC2	18	LLQs218PLz									
	19	RPAs314PEA									
	20	FPDs354RPA									
	21	GVNt393CDI									
	22	HQFs532FSP									
	23	FSFs534PER									
CDC27	24	TVLt203ETP									
	25	LTEt205PQD									
	26	LESs220NSK									
	27	KPKt264GRS									
	28	SVFs334QSG									
	29	FSQs336GNS									
	30	LSPt366ITs									
	31	TITs369PPN,									
	32	RLFt383SDS									
	33	LFTs384DSS									
	34	TSDs386STT									
	35	SDSs387TTK									
	36	SSTt389KEN									
	37	INDs426LEI									
	38	LDSs435IIS									
	39	SIIs438EGK									
	40	KISt444ITP									
	41	STIt446PQI									
	42	VALs553VLS									
	43	ALDt691LNK									
APC4	44	EVLs777ESE									
APC5	45	PMMt15NGV									
	46	LDVs195VRE									
	47	QAs221LLK									
	48	KALt232PAS									
	49	VASs674AAS									
APC6	50	NIIs559PPW									
	51	TGLt580PLE									
	52	LETs585RKT									
APC7	53	LTMs30NNN									
	54	SASt92PQS									
	55	LLSs22LLL									
	56	LLLt28MSN									
CDC23	57	KALs278IFN									
	58	QGEt556PTT									
	59	TPTt559EVP									
	60	ASLs572ANN									
	61	ANNt576PTR									
	62	RRVs582PLN									
	63	SSVt590P									
APC10	64	MTt3PNK									
CDC20	65	PAPs41PMR									
	66	EVAs92FLLS									
BUBR1	67	HILs367TRK									
	68	LLTs435AEK									
	69	KNKs543PPA									
	70	KKLs670PII									
	71	KLTs1043PGA									
Total			5	2	4	18	33	19	31	26	37

The green shading shows the presence of the phosphorylation site, and the white indicates the absence of a phosphorylation site.

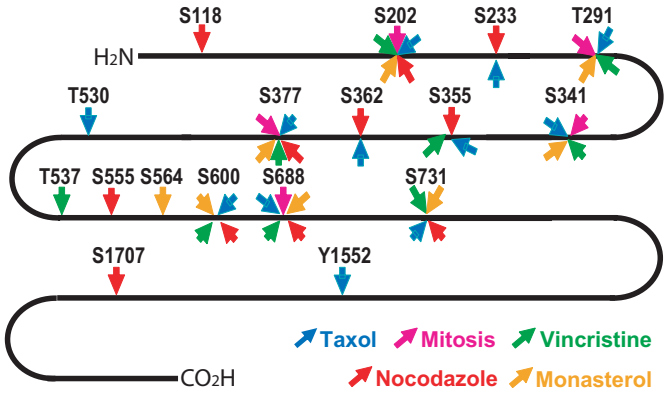

Fig. 1. A diagram depicting the phosphorylation sites identified on APC1 during drug-induced mitotic arrest. The arrows are color coded according to the drug treatment, and the number above the site indicates the site of phosphorylation.

compared phosphorylation in the nocodazole arrested cells with that in a set of cells undergoing mitosis, but not arrested in mitosis. We compared cells from double thymidine arrest released for 6–8 h. These cells had a robust mitotic index of 70%, compared with 90% for nocodazole arrest. However, the spectrum of phosphorylation was very different for some APC subunits but similar for others. In the mitosis samples, APC1 was phosphorylated at 5 sites, as compared with 11 for nocodazole arrest. Only 3 of the phosphorylation sites are common between the two conditions. The phosphorylation state for CDC27, APC4, and CDC16 were more similar between treatments. It is interesting to note that the subunits that showed the most similarity in phosphorylation between drug treatments contain protein interaction domains such as TPRs (tetratrico peptide repeats) and WD40 repeats.

Different Spindle Poisons Give Different Qualitative Phosphorylation Patterns. We then extended our analysis to other mitotic poisons. As shown in Fig. 1, a compilation of phosphorylation site data for the largest APC subunit, APC1, shows very different patterns of phosphorylation for different spindle poisons. Whereas several phosphorylation sites are shared among the treatments, such as Ser-202, Ser-377, and Ser-688, there are sites that seem to be specific to certain drugs. For example, Ser-233 is seen to be phosphorylated in nocodazole and taxol but not vincristine or monastrol, whereas Ser-1552 is specific for taxol arrest. Because samples were analyzed more than once, we were able to establish reproducibility. All of the phosphorylation sites listed were found in more than one analysis of the same treatment.

Although these differences were reproducible, there is still some concern about the threshold of detection. Phosphorylation sites that are basally phosphorylated at a very low stoichiometry are sometimes detected by mass spectrometry, whereas phosphorylations with high stoichiometries may not be detected, perhaps because the phosphopeptide coelutes with other peptides, resulting in undersampling. Although the samples were handled identically and we monitored the total amount of protein injected for each LC/MS analysis, we could not rule out relative differences in protein concentration, a crucial factor in determining the number of phosphorylation sites observed. Thus, to determine whether the differences we observed are real, we needed to provide a quantitative measure of phosphorylation that is comparable among drug treatments.

Quantitative Studies Confirm That Phosphorylation Patterns Resulting from Different Drug Treatments Are Distinct. Determining the degree of phosphorylation by mass spectrometry would be easy if an unmodified peptide and its phosphorylated cognate had the same

Table 2. A heat map of the quantitative measurements of phosphorylation stoichiometries of the sites found for each treatment followed by an 8-h release into mitosis

Protein	#	Phos. Motif	mn	n	t	vc	m
APC1	2	PPGs202PRE	0	0	0	0.17	0
	4	QGGt291PQN	0.03	0.6	0.03	0.1	0.02
	5	HSRs341PSI	0.15	0.9	0.29	0.1	0.01
	8	HNQS377PKR	0	0.14	2	0.75	0.02
	13	LELs600NGS	0.04	0.2	0	0.02	< 0.01
	14	GSLs688PVI	0.03	2.2	1	0.63	0.84
	15	LzLs731PSE	0	0	∞	0.4	0.01
APC2	18	LLQs218PLz	0.07	0.8	2.5	0.29	0.19
	19	RPAs314PEA	1.2	2.8	75	1.3	0.9
	22	HQFs532FSP	<0.01	0.23	0.23	0.14	0.14
	23	FSFs534PER	0.03	0.2	0.07	0.04	0.08
CDC27	25	LTEt205PQD	0.2	1.2	0.5	0.14	0.09
	26	LESs220NSK	1	0.4	0	0.2	0.1
	27	KPKt264GRS	1	0	no	0	1
	28	SVFs334QSG	0.1	0.3	0.3	0.7	0.2
	28 & 29	VFs334QSG FSQs336GN	0	12	0	0	0
	32 or 34	RLFt383SDS TSDs386STT	0	0.3	0.32	0.13	0.11
	33	LFTs384DSS	0.04	0.3	0	0.02	0.02
	37	INDs426LEI	0.1	0.8	0.3	0.2	0.02
	38	LDSs435IIS	0.2	<0.01	0.3	0.4	0.13
	39	SIIs438EGK	0.01	0.25	0.02	0.18	0.25
	38 & 39	LDSs435IIS SIIs438EGK	0.01	0.12	0.04	0.09	0.05
	41	STIt446PQI	0.2	1.3	0.7	0.6	0.2
APC4	44	EVLs777ESE	0.25	1.7	no	0.09	no
APC5	47	QAS221LLK	0	0.2	0	0.02	0
	48	KALt232PAS	0.09	0.08	0.04	0.08	0.14
CDC16	50	NIIs559PPW	0.15	2.9	0.05	1.45	<0.01
	51	TGLt580PLE	0.13	0.28	0.3	0.45	0.17
	51 & 52	TGLt580PLE PLEt585SRK	0.03	0.5	0	0.08	0.5
CDC23	58	QGEt556PTT	0.47	0.2	no	no	no
	62	RRVs582PLN	0.3	0.11	0.8	3.9	0.5
	62 & 63	RRVs582PLN SSVt590P	0	0.08	9	4.7	0.05

> 0.5
> 0.1
< 0.1
< 0.02
0
Pep & pPep not observed
signal too weak

mn, monasterol; n, nocodazole; t, taxol 20 mM; vc, vincristine; M, double thymidine.

flyabilities, as one could directly compare the signal intensities of these two species. However, we have recently found that using the same experimental conditions, the flyability ratio for a given peptide/phosphopeptide pair remains constant from experiment to experiment when the same peptide pair is examined (24, 25). Thus, reliable information about relative changes can be derived when the signals from identical peptides/phosphopeptide pairs are compared for the different drug treatments. To generate the data shown in Table 2, we determined which slices contained the protein of interest (SI Figs. 2–6 in *SI Appendix*); then we measured relative intensities of the phosphorylated peptides vs. their unphosphorylated complements. Not all of the 71 peptides mapped qualitatively provided good quantitative data. There are several explanations for this lack of signal. Most frequently, a single phosphorylation site was spread over multiple peptide species. This complication occurs when (*i*) there are multiple tryptic cleavage sites close together, resulting in a "ragged peptide"; (*ii*) the peptide contains e.g., a methionine residue that is easily partially oxidized; or (*iii*) the peptide is multiply modified. For 33 of the phosphorylation sites, we obtained reliable quantitative information for both the modified and unmodified peptides to determine the ratio of phosphorylated vs. unphosphorylated peptide.

CELL BIOLOGY

The phosphopeptide vs. peptide signal intensity ratio (Eq. **1**) allows for an easily accessible quantitative measure that can be compared between treatments. Here, I_{pP1} is the measured intensity of the phosphopeptide and I_{P1} is the intensity of the unphosphorylated cognate peptide, μ_{pP} is the flyability of the phosphopeptide, and μ_P the flyability of the unphosphorylated cognate peptide. $[pP_1]$ is the concentration of the phosphopeptide, and $[P_1]$ is the concentration of the unphosphorylated cognate peptide. The same equation was applied to another drug treatment for the same phosphopeptide/peptide pair in Eq. **2**. Thus, two drug arrest conditions can easily be compared as a ratio (Eq. **3**). It is obvious that the flyability ratios cancel out if the mass spectrometry conditions are kept similar such that the ratio of phosphopeptide vs. peptide signal intensity ratios is equivalent to the ratio of phosphopeptide vs. peptide concentration ratios (Eq. **4**).

$$\frac{I_{pP1}}{I_{P1}} = \frac{\mu pP[pP1]}{\mu P[P1]} \quad [1]$$

$$\frac{I_{pP2}}{I_{P2}} = \frac{\mu pP[pP2]}{\mu P[P2]} \quad [2]$$

$$\frac{I_{pP1}/I_{P1}}{I_{pP2}/I_{P2}} = \frac{\mu pP[pP1]/\mu P[P1]}{\mu pP[pP2]/\mu P[P2]} \quad [3]$$

$$\frac{I_{pP1}/I_{P1}}{I_{pP2}/I_{P2}} = \frac{[pP1]/[P1]}{[pP2]/[P2]} \quad [4]$$

This simple expression of the phosphorylation state facilitates the comparison between two or more drug treatments. The values for Eq. **1** are provided and the qualitative "heat map" shown in Table 2. The heat map shows the ratio of the signal intensity of the phosphopeptide to that of the unphosphorylated cognate. The color coding is as follows: red indicates a ratio of over 1, orange 1 to 0.1, dark yellow 0.1 to 0.02, and light yellow detectable levels below 0.02.

Table 2 shows clearly that the different qualitative patterns of phosphorylation for different drugs cannot simply be explained by differences in the sensitivity of the analysis between samples. For example taxol treatment gives high levels of phosphorylation (ratio >1) on six sites: APC1, Ser-377 (no. 8; ratio, 2), Ser-688 (no. 14; ratio, 1), Ser-731 (no. 15; ratio, ∞); APC2, Ser-218 (no. 18; ratio, 2.5), Ser-314 (no. 19; ratio, 75); and CDC23, Ser-582 (no. 62; ratio, 9). By comparison, vincristine treatment gives high levels of phosphorylation on only four sites. Although three of these sites are identical to those found in taxol arrest, one site is remarkably different: CDC16 (no. 50) Ser-559 is phosphorylated at a level of 1.45 in vincristine but only at 0.04 in taxol; CDC23 (no. 62) Ser-582 is phosphorylated at a level of 3.9 in the vincristine treatment and 0.8 in the taxol treatment. An even stronger contrast to vincristine and taxol is nocodazole vs. taxol. In nocodazole, seven sites are phosphorylated to a high degree and these sites are found on APC1, APC2 and CDC27 and CDC16. In general CDC27 is more highly phosphorylated in the nocodazole and vincristine treatments than it is in the taxol treatment. A few sites are highly phosphorylated among all or many of the treatments but not in the normal mitotic progression. These sites include the following: APC2, (no. 19) Ser-314; CDC27, (no. 25) Thr-205 (no. 37) Ser-426; CDC16, (50) Ser-559. Interestingly APC2, a core catalytic subunit that contains the cullin protein motif, shows the highest phosphorylation ratio of all of the sites observed. A remaining question is whether the patterns are stable or change over time.

Phosphorylation Patterns in Nocodazole-Arrested Cells Change Over Time. To study dynamic changes in phosphorylation patterns, quantitative measurements of phosphorylation that are accurate to <20% are needed. The error level of estimating the recovery of different peptides in multiple gel slices is too high for this kind of study. We therefore processed the entire sample after brief electrophoresis as a means of purification and immobilization without further fractionation. The complexity of the mixture reduced the number of peptides that could be identified; only 25 phosphopeptides were found using either Mascot or Protein Pilot.

On inspecting the initial data from a number of time points, several of the phosphopeptides seemed not to be at steady state. We used iQEM to look more closely at the quantitative kinetics of phosphorylation. Because peptides and their phosphorylated cognates have differential ionization/detection efficiencies, the phosphorylation stoichiometry cannot directly be derived from the relative peak intensities. However, although the ionization/detection efficiencies of a peptide/phosphopeptide pair are not known, their changes are correlated. This correlation enables one to calculate the ratio of flyabilities, which, in turn, allows one to derive the degree of phosphorylation based on the signal intensities when data for several samples with significantly different degrees of phosphorylation are available. We provided the proof of concept in two recent papers (24, 25) and introduce the term iQEM (isotope-free quantitation of the extent of modification) for this approach. iQEM allows us to determine the flyability ratio for a peptide/phosphopeptide pair, which in turn enables the calculation of the phosphorylation stoichiometry, not just a ratio of stoichiometries, which we used in the previous example; this estimate does not require the use of isotope-labeled standards. Instead of isotope-labeled standards, iQEM uses a set of peptides derived from the protein of interest, chosen because they do not show sample-to-sample variation and are therefore presumably unmodified, as omnipresent internal standards. By characterizing the properties of these peptides and then detecting their presence in our samples, we can normalize/correct for variations of the absolute amount of the target protein present in the extract. Because we can then assume conservation of mass we can calculate the ionization/response factors as the decrease of the one signal, e.g., the peptide is correlated with the increase of the cognate signal of the phosphopeptide (24).

In this case, four or five standard peptides were used per protein for normalization. We chose our normalization peptides by looking at peptides that gave ion currents variations among the samples that reflected the general variations of the majority of the peptides. To illustrate the method, the expected behavior of peptides from a single protein measured over several time points is shown in a diagram (SI Fig. 7 in *SI Appendix*). Blue lines represent peptides that are not modified in the biological condition under study; these peptides show a similar pattern over the time course, with the intensities measured depending largely on the amount of sample injected onto the HPLC column. Black lines show peptides that are modified during the time course; these "black" peptides start out following the same pattern as the blue lines, but sharply diverge at some point. The green and yellow lines show the concomitant increase of the corresponding modified peptides. In every LC/MS time course there will be some peptides that show an aberrant intensity pattern (red lines). These peptides often contain e.g., methionine, which undergoes unpredictable oxidation.

Using well behaved peptides (blue lines) we can accurately normalize phosphorylated and unmodified peptides through a simple calculation. The phosphorylation stoichiometry can be determined based on the relative ion signal intensities of the two species after correcting for the different response factors by knowing the flyability ratio of a peptide/phosphopeptides pair calculated based on the conservation of mass (for details, see ref. 24). The flyabilities can be very different for the phosphorylated and unphosphorylated forms. Therefore, the uncorrected ion currents are unreliable for determining the precise amount of peptide present. In Fig. 2*A*, for example, CDC16 peptide NIIs559PPWDFR displays a remarkable 60-fold increase in the intensity of the phosphopep-

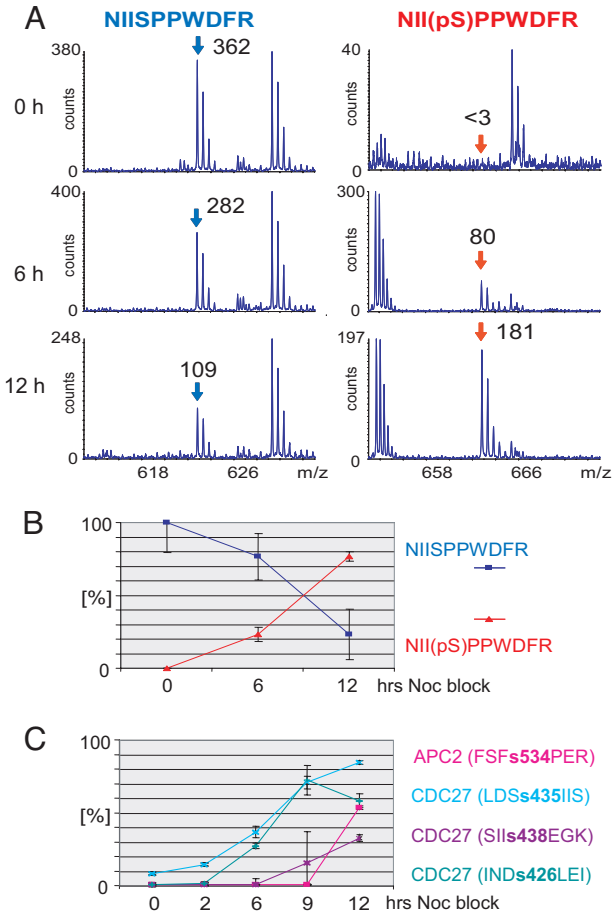

Fig. 2. Stable isotope free quantitation of the extent of phosphorylation. (*A*) Mass spectra of the CDC16 peptide NIISPPWDFR and its phosphorylated counterpart at the 0-, 6-, and 12-h time points. The given numbers correspond to the peak intensities after averaging over the elution time window. (*B*) Graphical representation of the increase/decrease of NIIpSPPWDFR and NIIS-PPWDFR. (*C*) A plot of the phosphorylation stoichiometries of four different phosphorylation sites (APC2, S534; and CDC27, S426, S435, and S438) as determined by using the iQEM approach. Clearly, different kinetics of phosphorylation are observed.

tide and only a 3-fold decrease for the unphosphorylated cognate. Without iQEM normalization this result is uninterpretable, but using iQEM we find that the stoichiometry of increase and decrease is exactly complementary (Fig. 2*B*). Phosphorylation at that site increases from 0% to 80% and the cognate unphosphorylated peptide decreases from 100% to 20%. We give additional examples of such peptides in SI Figs. 8 *a*nd 9 in *SI Appendix*.

Using this method, we can show that in nocodazole arrest, APC phosphorylation changes significantly over time. Dynamic changes in phosphorylation levels for four different phosphorylation sites, one on APC2 and three on CDC27, are shown in Fig. 2*C*. Each site shows different kinetics. The rate of phosphorylation at Ser-426 on CDC27 steadily increases until the 9-h time point, whereas that at Ser-435 increases more rapidly from 2 to 8 h and then the rate of phosphorylation decreases. This decrease in the rate of Ser-435 phosphorylation is coincident with the detection of a second phosphorylation site on Ser-438, manifested by the detection of the doubly phosphorylated peptide species Phosphorylation at the Ser-534 site on APC2 is undetectable until the 12-h time point. We show other peptides quantitated in a similar fashion in SI Figs. 10 and 11 in *SI Appendix*. Thus, quantitative measurements show that nocodazole "arrest" is not a static state: APC phosphorylation patterns change significantly depending on the duration of the arrest.

Discussion

We studied three aspects of the phosphorylation patterns on the 11 core proteins of the APC plus interactors: (*i*) qualitative phosphorylation mapping, (*ii*) relative quantitation to detect differences, and (*iii*) where necessary, quantitation in actual stoichiometries by iQEM. We used standard methods to identify 71 sites of phosphorylation, under a variety of conditions, and we were also able to use nonnormalized ion currents to compare phosphorylation levels for a subset of these sites at different points in the cell cycle and in mitotic arrest in response to antimitotic drugs. Neither of these approaches was sufficiently quantitative to measure kinetic features of phosphorylation. For that, we used a recently developed iQEM technique, which provides accurate absolute stoichiometry without using isotope-labeled standards.

Using these methods, we were able to uncover differences between the mitotic arrest states imposed by different spindle poisons and distinguish between these states and the normal metaphase condition. We also found that mitotic arrest in response to the spindle poison nocodazole is a dynamic, not a static, state.

Drug-Arrested Mitotic States Are Not a Faithful Reflection of Normal Mitosis. Our analysis of the phosphorylation state of the APC at different cell cycle stages allowed us to show that the pattern of phosphorylation in prometaphase arrest by nocodazole was significantly different from that of cells synchronized in mitosis after timed release from double thymidine block. We considered two different explanations for this disparity. The first possibility is that nocodazole might arrest cells at a specific short-lived point in the mitotic cycle, which we might have missed in our studies of the synchronized but unarrested cell cycle. The semiquantative data on nocodazole arrest, suggest that this explanation is unlikely. For example Thr-205 (25) on CDC27 showed a phosphorylation level in nocodazole of 1.2 whereas that same site in the mitotic state was 0.09. Such a high phosphorylation level could only be masked if the state stabilized by nocodazole represents <4% of the time spent in normal mitosis (90 min); such extremely rapid changes in phosphorylation seem unlikely. Similarly Ser-221 (no. 47) in APC5 had a ratio of 0.2 but was undetectable in the normal mitotic cells.

A second explanation might be that the nocodazole state of arrest is not a subset of mitosis but a specific response to microtubule depolymerizing drugs. If this explanation were true then a similar response would be expected for vincristine, which is also a microtubule depolymerizing agent. Vincristine arrest does show six of the same phosphorylation sites on APC1 as nocodazole, but we also found a number of unique sites (five for nocodazole and four for vincristine). We cannot attribute the difference between nocodazole and vincristine to peptides that were systematically missed in the different analyses, because we observed each corresponding unphosphorylated peptide in both sets of samples and the analyses were repeated.

It is clear that the nocodazole-arrested state, at least as reflected in APC phosphorylation, does not represent a well populated state found in normal mitosis. Although all of the phosphorylations found in mitosis are also observable in the drug arrest, we find many specific to the drug-arrested state. Further work will be required to determine the causes and effects of these extra phosphorylations.

Mass Spectrometry Offers a Way of Examining the Differences Between Different Spindle Poisons. Some drugs that bind to microtubules and block mitosis are ineffective in cancer treatment; others show inexplicable focal efficacy. For example, the vinca alkaloids are useful for treating lymphoma, neuroblastoma and nephroblastomas, whereas taxol is useful for advanced breast cancer and ovarian cancer. We do not know why these drugs are not all equally effective, nor why they have different therapeutic value against

different cancers. It is possible, perhaps likely, that our observations of distinct phosphorylation states of the APC in response to different antimitotic drugs may point to an explanation of some of these differences. Furthermore, it is possible that cells from different tissues, or cells harboring different mutations, or cells under different physiological stresses, such as hypoxia, may differ in their response to spindle poisons and would reflect those differences in different sites of phosphorylation. In that respect, differences in spindle checkpoint phosphorylation may reveal new features of the mitotic state.

It is also possible that antimitotic agents differentially affect the activity of kinases, such as CDK1 and aurora B, leading to variations in spindle checkpoint responses. The ability to characterize drug candidates based on the spectrum of APC phosphorylations may facilitate the categorization of drugs, the discrimination of the response of tumors to drugs, and the identification of new means of checkpoint control.

Dynamics of Phosphorylation. Our results emphasize the fact that mitotic arrest is a misnomer: arrest is a dynamic state in which some cells enter apoptosis and other cells revert to interphase. The ability to observe biochemical events during arrest could be very important for understanding antiproliferative treatments. However, exploring the dynamics of phosphorylation makes great demands on the accuracy of quantitation. Most mass spectrometric based quantitative approaches, including SILAC and iTRAQ, give relative data, meaning that one state of phosphorylation is determined relative to another phosphorylation state (26–28); these data are insufficient to establish the kinetics of a pathway. iQEM offers a significant advance over earlier techniques. It has allowed us to measure specific quantitative changes in APC phosphorylation in cells arrested in nocodazole for varying periods. Although we do not yet understand the specific dynamics that we have discovered here, they are intriguing. If these dynamics can be correlated with the process by which the arrested state is resolved, they may provide us with new tools to understand the mitotic process and to find more effective drug targets in cancer.

Materials and Methods

Chemicals. All chemicals, if not otherwise stated, were purchased from Sigma–Aldrich (St. Louis, MO). HPLC-grade solvents for mass spectrometric analyses were acquired from Burdick and Jackson (Morristown, NJ).

Preparation of Synchronized HeLa Cell Extracts. HeLa S3 cells were obtained from ATCC. Cells were grown in spinner flasks in Dulbecco's modified Eagle's medium (DMEM) supplemented with 10% FBS and 100 μg/ml penicillin/streptomycin. Cells were synchronized at the G_1/S transition by double thymidine block as previously described. Details of the antimitotic drug treatments are described in the supplementary materials. All cultures were analyzed by FACS to ensure the correct cell cycle state. Cell extracts were prepared by lysing the cell pellet in 1 vol of PBS buffer supplemented with 0.1% Triton X-100, 1 nM okadaic acid, 1 μg/ml microcystine-LR (Alexis Biochemicals), 10 mM sodium fluoride, and 10 μg/ml each of chymostatin, pepstatin, and leupeptin. The cells were passed through a 27-gauge needle to shear the DNA. The extract was precleared by centrifugation for 20 min at 20,000 $\times$ g at 4°C.

Immunoprecipitation of APC from Extracts. The APC was immunoprecipitated by using the anti-CDC27 antibody sc-6392 (Santa Cruz). Details of the procedure are described in *SI Appendix*.

Time Course Experiments. Cells were synchronized by using a double thymidine arrest in G_1/S phase as previously described and fresh medium was added after the cells were washed. After 4 h, nocodazole was added to the cells. Time points were taken at 0, 3, 6, 8, 10, and 12 h. This particular experiment was repeated three times with varying time points to gauge the time windows for appropriate measurements. Phosphorylation sites on CDC27 were used to check the reproducibility of the kinetics between experiments. Immunoprecipitations were performed as described above and the samples were run into a 10% gel but not separated. The protein was then in-gel digested and analyzed by using LC/MS.

Mass Spectrometry. All experiments were performed by using a QSTAR XL mass spectrometer (Applied Biosystems/MDS Sciex, Concord, Canada) coupled to a microscale capillary HPLC (Famos microautosampler; LC Packings, Sunnyvale, CA), Agilent 1100 HPLC pump (Agilent, Andover, MA)). Columns (length, 15 cm; inner diameter, 75 μm) were packed in-house by using Magic C18 beads (Michrom BioResources, Auburn, CA). Buffer A was 2.5% acetonitrile/0.2% formic acid; buffer B was 97.3% acetonitrile/0.2% formic acid.

ACKNOWLEDGMENTS. We thank Ron Bonner, Lyle Burton, and Keith Ashman for helpful discussions. This work was supported by National Institutes of General Medical Sciences Grant GM039023.

1. King RW, *et al*. (1995) A 20S complex containing CDC27 and CDC16 catalyzes the mitosis-specific conjugation of ubiquitin to cyclin B. *Cell* 81:279–288.
2. Shteinberg M, Protopopov Y, Listovsky T, Brandeis M, Hershko A (1999) Phosphorylation of the cyclosome is required for its stimulation by Fizzy/cdc20. *Biochem Biophys Res Commun* 260:193–198.
3. Fang G, Yu H, Kirschner MW (1998) Direct binding of CDC20 protein family members activates the anaphase-promoting complex in mitosis and G1. *Mol Cell* 2:163–171.
4. Kraft C, *et al*. (2003) Mitotic regulation of the human anaphase-promoting complex by phosphorylation. *EMBO J* 22:6598–6609.
5. Kotani S, Tanaka H, Yasuda H, Todokoro K (1999) Regulation of APC activity by phosphorylation and regulatory factors. *J Cell Biol* 146:791–800.
6. Yu H (2002) Regulation of APC-Cdc20 by the spindle checkpoint. *Curr Opin Cell Biol* 14:706–714.
7. Eckerdt F, Strebhardt K (2006) Polo-like kinase 1: Target and regulator of anaphase-promoting complex/cyclosome-dependent proteolysis. *Cancer Res* 66:6895–6898.
8. Sumara I, *et al*. (2004) Roles of polo-like kinase 1 in the assembly of functional mitotic spindles. *Curr Biol* 14:1712–1722.
9. van de Weerdt BC, *et al*. (2005) Uncoupling anaphase-promoting complex/cyclosome activity from spindle assembly checkpoint control by deregulating polo-like kinase 1. *Mol Cell Biol* 25:2031–2044.
10. Pinsky BA, Kung C, Shokat KM, Biggins S (2006) The Ipl1-Aurora protein kinase activates the spindle checkpoint by creating unattached kinetochores. *Nat Cell Biol* 8:78–83.
11. Rudner AD, Murray AW (2000) Phosphorylation by Cdc28 activates the Cdc20-dependent activity of the anaphase-promoting complex. *J Cell Biol* 149:1377–1390.
12. Peters JM, King RW, Hoog C, Kirschner MW (1996) Identification of BIME as a subunit of the anaphase-promoting complex. *Science* 274:1199–1201.
13. Lahav-Baratz S, Sudakin V, Ruderman JV, Hershko A (1995) Reversible phosphorylation controls the activity of cyclosome-associated cyclin-ubiquitin ligase. *Proc Natl Acad Sci USA* 92:9303–9307.
14. Tang Z, Bharadwaj R, Li B, Yu H (2001) Mad2-Independent inhibition of APCCdc20 by the mitotic checkpoint protein BubR1. *Dev Cell* 1:227–237.
15. Kramer ER, Scheuringer N, Podtelejnikov AV, Mann M, Peters JM (2000) Mitotic regulation of the APC activator proteins CDC20 and CDH1. *Mol Biol Cell* 11:1555–1569.
16. Kramer ER, Gieffers C, Holzl G, Hengstschlager M, Peters JM (1998) Activation of the human anaphase-promoting complex by proteins of the CDC20/Fizzy family. *Curr Biol* 8:1207–1210.
17. Horwitz SB (1992) Mechanism of action of taxol. *Trends Pharmacol Sci* 13:134–136.
18. Kolman A (2005) Activity of epothilones. *Curr Opin Investig Drugs* 6:616–622.
19. Manfredi JJ, Horwitz SB (1984) Taxol: An antimitotic agent with a new mechanism of action. *Pharmacol Ther* 25:83–125.
20. Wilson L, Bamburg JR, Mizel SB, Grisham LM, Creswell KM (1974) Interaction of drugs with microtubule proteins. *Fed Proc* 33:158–166.
21. Jordan MA, Wilson L (2004) Microtubules as a target for anticancer drugs. *Nat Rev Cancer* 4:253–265.
22. Kops GJ, Weaver BA, Cleveland DW (2005) On the road to cancer: Aneuploidy and the mitotic checkpoint. *Nat Rev Cancer* 5:773–785.
23. Pinsky BA, Biggins S (2005) The spindle checkpoint: Tension versus attachment. *Trends Cell Biol* 15:486–493.
24. Steen H, Jebanathirajah JA, Springer M, Kirschner MW (2005) Stable isotope-free relative and absolute quantitation of protein phosphorylation stoichiometry by MS. *Proc Natl Acad Sci USA* 102:3948–3953.
25. Steen H, Jebanathirajah JA, Rush J, Morrice N, Kirschner MW (2006) Phosphorylation analysis by mass spectrometry: Myths, facts, and the consequences for qualitative and quantitative measurements. *Mol Cell Proteomics* 5:172–181.
26. Zhang Y, *et al*. (2005) Time-resolved mass spectrometry of tyrosine phosphorylation sites in the epidermal growth factor receptor signaling network reveals dynamic modules. *Mol Cell Proteomics* 4:1240–1250.
27. Wolf-Yadlin A, *et al*. (2006) Effects of HER2 overexpression on cell signaling networks governing proliferation and migration. *Mol Syst Biol* 2:54.
28. Olsen JV, *et al*. (2006) Global, in vivo, and site-specific phosphorylation dynamics in signaling networks. *Cell* 127:635–648.